Poly-IGO TFT with Field-Effect Mobility over 40 cm^2/Vs – Mobility Modeling and Self-Heating Simulation –

Mutsumi Kimura*, Masato Hiramatsu*, Toshio Kamiya, Koji Yamaguchi***, Emi Kawashima***, Yuki Tsuruma*****

*Ryukoku University, Otsu, Japan
**Institute of Science Tokyo, Yokohama, Japan
***Idemitsu Kosan Co., Ltd., Sodegaura, Japan

Abstract

A poly-IGO TFT with field-effect mobility (μ_{FE})>40cm²/Vs has been analyzed, which is the highest among oxide semiconductor TFTs using common materials and mature production processes. The mobility modeling clarifies the intrinsic mobility positively depends on the carrier density, and the self-heating simulation clarifies it slightly positively depends on the temperature, which enhance μ_{FE}. We expect α-IGZO TFTs can be replaced in the near future.

Author Keywords

Polycrystalline In-Ga-O (poly-IGO), Field-effect mobility (μ_{FE}), Mobility modeling, Self-heating simulation

1. Introduction

Metal-oxide semiconductor (OS) thin-film transistors (TFT)[1,2] not only have been widely utilized in electronic displays, such as, liquid-crystal displays (LCD), organic light-emitting diode displays (OLED), micro LEDs (μ-LED), etc., as active-matrix devices, but also being investigated in emerging applications, such as, dynamic random access memory (DRAM) as switching devices, back end of line (BEOL) as power devices, etc. However, more and more high performance, such as, field-effect mobility (μ_{FE}) over several tens cm²/Vs, are needed for large-area, high-resolution, or fast-refresh-rate displays[3] and for dramatically improvement of the emerging applications, which is difficult to achieve among conventional OS TFTs. In our study, a polycrystalline In-Ga-O (poly-IGO) TFT with μ_{FE} over 40 cm²/Vs has been developed and analyzed by mobility modeling and self-heating simulation. The μ_{FE} is the highest among OS TFTs using common semiconductor materials and mature production processes. In this presentation, the mobility modeling and self-heating simulation will be explained in detail. They will clarify that the intrinsic carrier mobility (μ) positively depends on the carrier density (n) and temperature (T), which enhances the μ_{FE}. Because of these characteristics, it is expected that poly-IGO TFTs can replace amorphous In-Ga-Zn-O (α-IGZO) TFTs in the near future.

2. Poly-IGO TFT

The poly-IGO TFT is shown in Fig. 1. The device structure is shown in Fig .1(a). First, on a glass substrate and SiO_2 buffer layer, IGO is deposited by DC magnetron sputtering as an oxide channel layer, whose thickness is 30 nm, patterned, and then crystallized by furnace annealing in air at 400 °C, which is the highest temperature in the production processes, and therefore the poly-IGO TFTs can be fabricated on glass substrates and in BEOL. Next, SiO_2 is deposited as a gate insulator layer, whose thickness is 100 nm, molybdenum is deposited as a gate electrode layer, and they are patterned. Then, SiO_2 is again deposited as an interlevel dielectric layer, which automatically forms low resistance regions in the oxide channel layer, whose sheet resistance is as low as 418 Ω/□, and a self-align structure. Finally, molybdenum is again deposited on the low resistance regions as a source and drain electrode layer.

The Ids-Vgs characteristic and μ_{FE} are shown in Fig. 1(b). Here, the μ_{FE} is obtained from an equation of Ids in the linear region for Vds=0.1 and from that in the saturation region for Vds=10 and 20. It is found that the maximum value of the μ_{FE} is 40.1 cm²/Vs for Vds=0.1 and 44.7 for Vds=20. As aforementioned, the μ_{FE} is the highest among OS TFTs using common semiconductor materials and mature production processes.

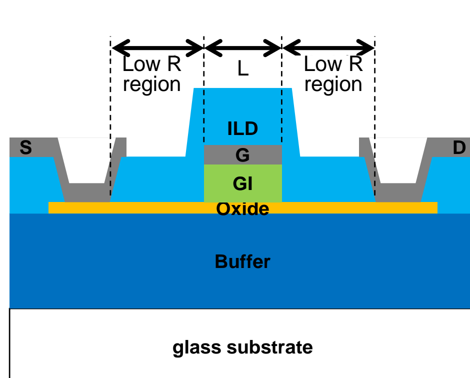

(a) Device structure.

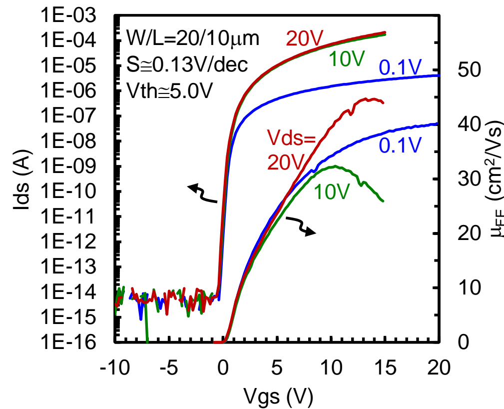

(b) Ids-Vgs characteristic and μ_{FE}.

Figure 1. Poly-IGO TFT.

ISSN 0097-996X/25/5602-0836-$1.00 © 2025

3. Mobility Modeling

Trap Extraction: The trap extraction is shown in Fig. 2. Here, a low-frequency (f) Cg(s+d)-Vg(s+d) characteristic is utilized to extract a trap density[4]. The extraction method that we developed has an outstanding advantage that the trap density can be extracted only by the low-f Cg(s+d)-Vg(s+d) characteristic without the Ids-Vgs characteristic, which enable mobility modeling later. The low-f Cg(s+d)-Vg(s+d) characteristic is shown in Fig. 2(a). It is found that the characteristic plots do not shift any further even when the f decreases below 1 Hz, which indicates a quasi-static condition can be acquired at 1 Hz.

Mobility Modeling: The mobility modeling is shown in Fig. 3. The measured Ids, which is the same as that in Fig. 1(b), vs extracted carrier density per unit area (n_a), which is extracted during the trap extraction, are shown in Fig. 3(a). It is found that the Ids plot is concave, whereas the n_a plot is linear, and therefore it is suggested that the μ depends on n.

The modeling procedure is shown in Fig. 3(b). Briefly speaking, the μ is obtained one by one for each n to reproduce the Ids[5]. Because the n varies along the depth in the oxide channel layer, the modeling method is complicated, but we have successfully developed it. The Ids is composed of the sum of the electric

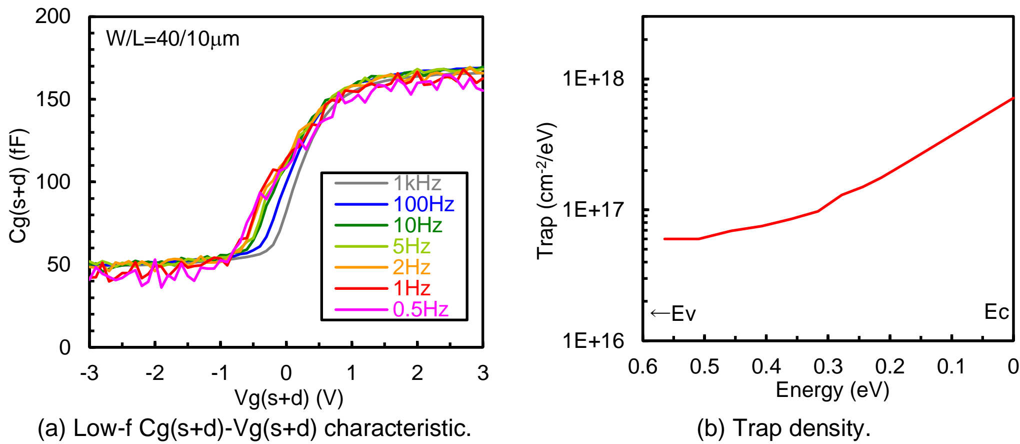

(a) Low-f Cg(s+d)-Vg(s+d) characteristic. (b) Trap density.

Figure 2. Trap extraction.

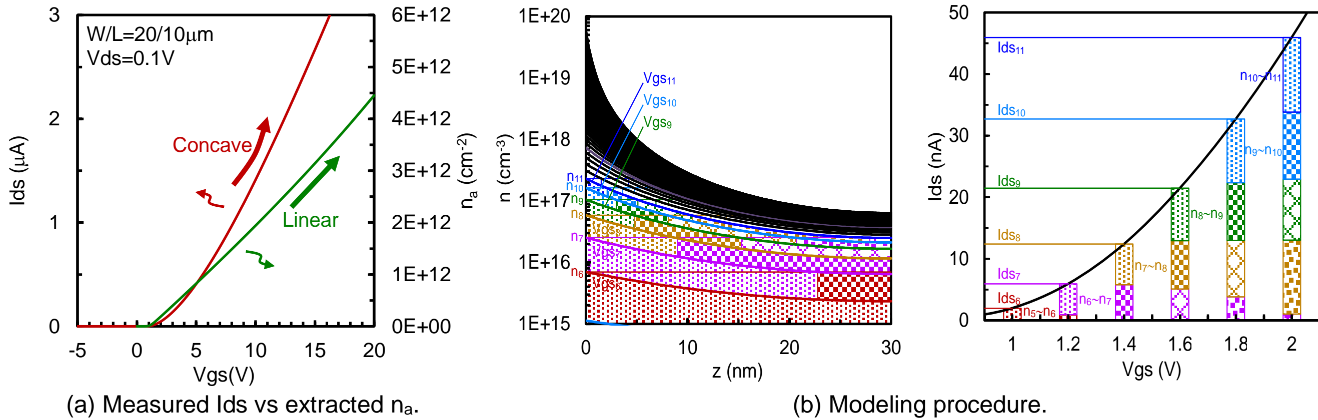

(a) Measured Ids vs extracted n_a. (b) Modeling procedure.

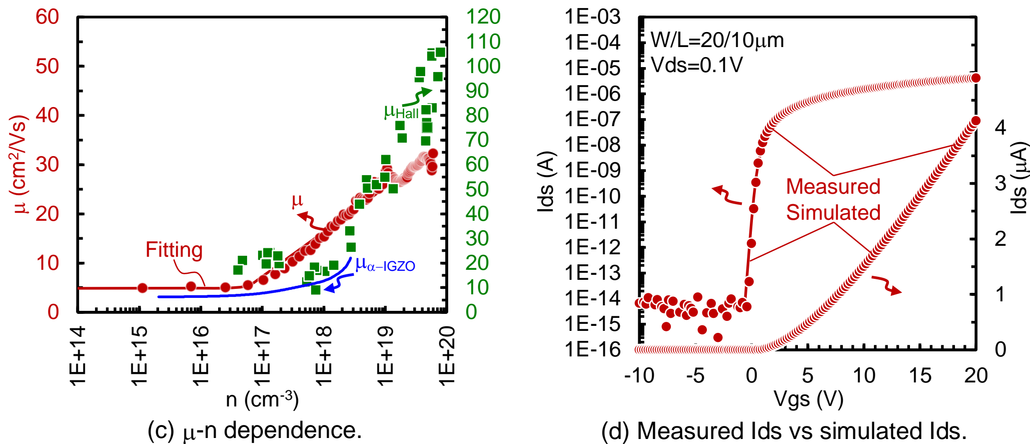

(c) μ-n dependence. (d) Measured Ids vs simulated Ids.

Figure 3. Mobility modeling

current for each n and corresponding μ along the channel layer depth.

$$I_{ds_i} = \kappa \int \mu(n) \cdot n \cdot dz \cong \kappa \sum_{j=1}^{i} \mu_j \cdot n_j \cdot \Delta z \quad (1)$$

Here, *i* is the turn of each Vgs application, $\kappa = (W/L)V_{ds}$ z is an axis along the channel layer depth. So, the μ_i is inductively obtained so that the calculated Ids is equal to the measured Ids in the following equation.

$$I_{ds_i} \cong \kappa\left(\sum_{j=1}^{i-1} \mu_j \cdot n_j \cdot \Delta z + \mu_i \cdot n_i \cdot \Delta z\right) \quad (2)$$

The μ-n dependence is shown in Fig. 3(c). Here, the obtained μ and fitting line are shown. It is found that the μ is low and constant below n = 10^{17} cm^{-3}, whereas it increases linearly above that, which may be due to a behavior of potential barriers at grain boundaries[6]. Namely, the μ positively depends on the n, which enhances the μ_{FE}, because the Ids is pushed up greater as n increases. The μ-n dependence can be a universal curve, which is well-known for conventional silicon but has not been previously reported for poly-OS semiconductors, and indispensable to design devices and circuits in the future. Moreover, Hall mobility (μ_{Hall}) is also overlaid in this figure. It should be noted that the rough shape is similar, namely, the μ_{Hall} is low and constant below a certain n, whereas it increases linearly above that, but the values of n and μ_{Hall} is different. The fact that μ is lower than μ_{Hall} is likely due to the decrease in mobility caused by the differences in the device fabrication process from the single film. In poly-OS, mobility significantly changes depending on the differences in the TFT fabrication process[7]. These show that actually fabricating TFTs and modeling the mobility using this method are important. Furthermore, the intrinsic carrier mobility for α-IGZO ($\mu_{\alpha\text{-IGZO}}$) is also overlaid in this figure. It is found that the shape and value are quite different, which again guarantees that the μ-n dependence is due to the behavior of potential barriers at grain boundaries and in-grain scattering such as neutral impurity scattering and ionized impurity scattering, because α-OS including the α-IGZO and α-IGO has no grain boundaries and large impurity scattering[8].

The measured Ids vs simulated Ids, which is simulated by employing a device simulator and implementing the μ-n dependence, is shown in Fig. 3(d). It is found that they completely overlap, which guarantees the perfect validity of the mobility modeling.

4. Self-Heating Simulation

T-dependent μ: The T-dependent Ids-Vgs characteristic is shown in Fig. 4. It is unclear in the Ids-Vgs characteristic but clear in g_m-Vgs characteristic. It is found that the g_m is larger when the T is higher below Vgs = 10 V, whereas vice versa above that.

The T-dependent μ-n dependence is shown in Fig. 5. Here, the modeling procedure is the same as that mentioned in the last chapter, the fitting lines are obtained for each T, and they are smoothly interpolated and extrapolated as a function of n and T.

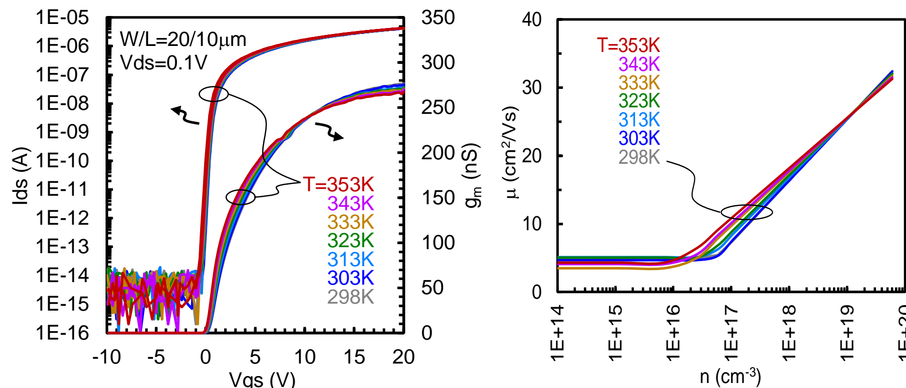

Figure 4. T-dependent Ids-Vgs characteristic.

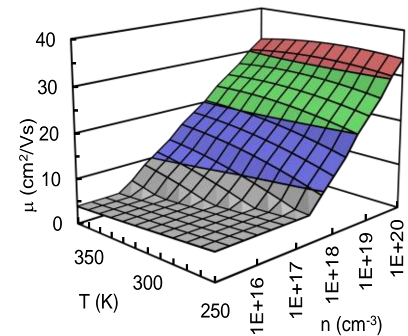

Figure 5. T-dependent μ-n dependence.

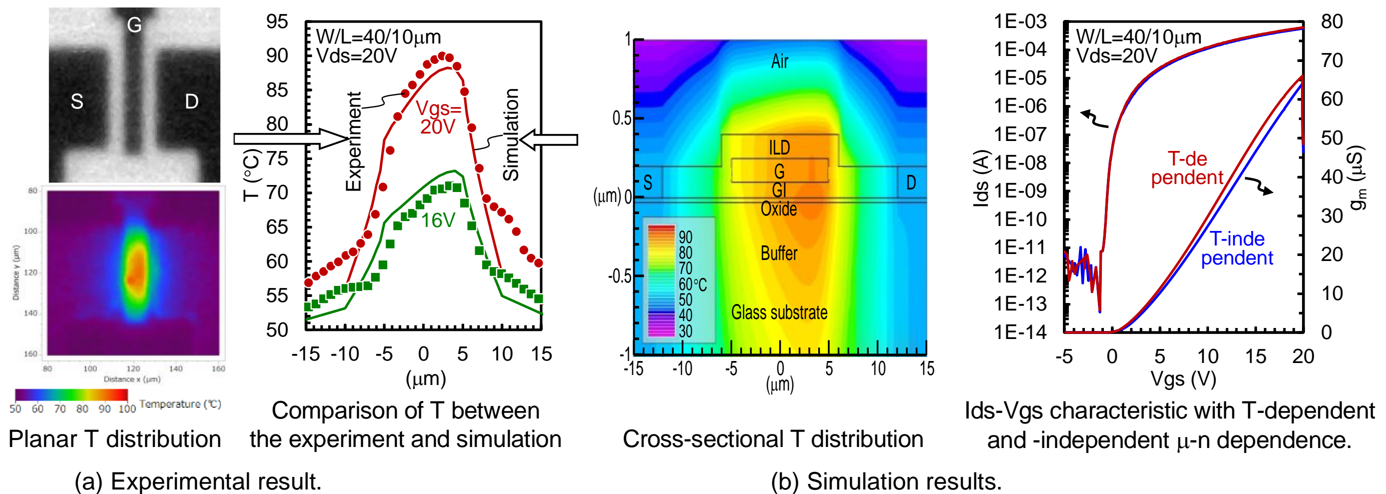

Planar T distribution

Comparison of T between the experiment and simulation

(a) Experimental result.

Cross-sectional T distribution

Ids-Vgs characteristic with T-dependent and -independent μ-n dependence.

(b) Simulation results.

Figure 6. Self-heating effect.

The T-dependent μ-n dependence can be also a universal curve and indispensable to design devices and circuits in the future.

Self-heating Simulation: The self-heating effect is shown in Fig. 6. The experimental result is shown in Fig. 6(a). Here, the planer T distribution is measured by employing an infrared microscope. It is found that T increases to roughly 90 °C sharply on the oxide channel layer.

The simulation result is shown in Fig. 6(b). Here, the cross-sectional T distribution is simulated by employing the device simulation with a thermal analysis module. It is found that T is roughly the same between on the channel and surface, which guarantees that the planer T distribution of the experimental result as in Fig. 6(a) reflects that in the channel layer. Incidentally, the comparison of T between the experiment and simulation assures the validity of the simulation. Moreover, the Ids-Vgs characteristic with T-dependent and -independent μ-n dependence is shown. It is found that the g_m is larger for that with the T-dependent μ-n dependence. Namely, the μ slightly but positively depends on the T, which enhances the μ_{FE}, because the Ids is pushed up as T increases owing to the self-heating effect.

5. Conclusion

A poly-IGO TFT with μ_{FE} over 40 cm^2/Vs has been analyzed by mobility modeling and self-heating simulation. The μ_{FE} is the highest among OS TFTs using common semiconductor materials and mature production processes. First, the mobility modeling clarified that the μ positively depends on the n, which enhances the μ_{FE}. Moreover, the self-heating simulation clarified that μ slightly but also positively depends on the T, which also enhances μ_{FE}. The T-dependent μ-n dependence can be a universal curve and indispensable to design devices and circuits. Because of these characteristics, it is expected that poly-IGO TFTs can replace α-IGZO TFTs in the near future.

6. Acknowledgements

The authors gratefully acknowledge the contributions of Dr. Yukiharu Uraoka, Dr. Takanori Takahashi, and Dr. Ryoko Miyanaga of NAIST.

7. References

1. Nomura K, Ohta H, Ueda K, Kamiya T, Hirano M, Hosono H. Thin-film transistor fabricated in single-crystalline transparent oxide semiconductor. Science. 2003 May; 300: 1269-1272.
2. Nomura K, Ohta H, Takagi A, Kamiya T, Hirano M, Hosono H. Room-temperature fabrication of transparent flexible thin-film transistors using amorphous oxide semiconductors. Nature. 2004 Nov; 432: 488–492,.
3. Matsueda Y. Required characteristics of TFTs for next generation flat panel display backplanes. in Proc The 6th International Thin-Film Transistor Conf. 2010; 314,.
4. Kimura M, Nakanishi T, Nomura K, Kamiya T, Hosono H. Trap densities in amorphous-$InGaZnO_4$ thin-film transistors. Appl Phys Lett. 2008 Apr; 92(13): 133512.
5. Kimura M, Kamiya T, Nakanishi T, Nomura K, Hosono H. Intrinsic carrier mobility in amorphous In-Ga-Zn-O thin-film transistors determined by combined field-effect technique. Appl Phys Lett. 2010 June; 96(26): 262105.
6. Kimura M, Inoue S, Shimoda T, Sameshima T. Device simulation of carrier transport through grain boundaries in lightly doped polysilicon films and dependence on dopant density. Jpn J Appl Phys pt. 1. 2001 Sept; 40(9R): 5237-5243, .
7. Tsubuku M, Watakabe H, Sasaki T, Tamaru T, Onodera R, Mochizuki M, Kimura H, Kawashima E, Sasaki D, Tsuruma Y. High mobility poly-crystalline oxide TFT achieving mobility over 50 cm^2/Vs and high level of uniformity on the large size substrates. In SID 2023 Digest. 2023 May; 78-81,.
8. Tsuruma Y, Nagatomi H, Iwase N, Yamaguchi K, Sasaki D, Kawashima E, Kaijo A, Inoue K. Poly-OS IGO for high mobility TFT applications. In MRM 2023 / IUMRS-ICA 2023 Digest. 2023 Dec; S2-O202-02.